

# Leaky Dams

Rob Gondris

21 September 2020

## 1 Summary

In this project, we investigate the effectiveness of Leaky Dams for flood prevention, specifically for large catchments. We model the potential effectiveness of these Leaky Dams, and compare it to the results found for smaller catchment sizes.

This project extends the ideas presented in Hankin et al, 2020. We first derive a system of ordinary differential equations that model river flow, where one dam can be placed in each segment. We then write code that gives a numerical solution. We apply this to a large catchment in Cumbria, UK. We investigate the results and show how dam design affects performance, and highlight the potential benefits and drawbacks of using a model to specify dam design.

## 2 Introduction

There is a growing interest in ‘Leaky Dams’, a low cost nature-based flood barriers. These are intended to be located on upstream branches in a river catchment. They are part of the UK Government’s plan for working with natural processes to reduce flood risk (Environment Agency, [2]), and are often contained in nature based approaches to flood prevention (Nicholson, 2020).

Leaky dams are designed to simulate fallen trees and are often built to be permeable. This means that they have little affect on the stream if the flow through them is small, however they hold back more water as the flow through them increases. An example is shown in Figure 1. They are currently seen by the UK government as an additional prevention measure, and not as a replacement for traditional flood prevention strategy (GOV.UK [4]). In this project, we modify the approach taken in Hankin et al, 2020. We model the river as a series of uniform segments, and derive a system of differential equations to model how the flow evolves. These will be solved numerically in Python. The code is explained with worked examples. We also give various methods of visualising the results. The code is presented in Jupyter notebooks in GitHub<sup>1</sup>.

The model is then applied to a large catchment, the source of the river Kent in Cumbria, Britain. The Kent is prone to flooding, for example during storm Ciara in February 2020 (BBC [10]). We model what effect different dam set-ups have, and how the design of the dams influence their effectiveness.

---

<sup>1</sup><https://github.com/robgondris/network-flood-model>



Figure 1: Leaky dam near Reston, Scotland. Jayne Wilkinson (South Cumbria Rivers Trust)

### 3 Derivations

#### 3.1 Overview

A river network is modelled as a set of idealised segments, where flow is uniform within each segment. A key property of a leaky dam is that it should not have a large impact on a segment if there isn't much water flowing through it. We use a simple model for a dam, by allowing the base of the dam to be a set height above the segment base. The following model is an extension of the one in Hankin et al 2020. We use two different methods for solving the system of differential equations and compare the two. A mathematically derived model is necessary because there is a lack of empirical data for leaky dams (although this has since been addressed see Follett et al, 2020).

#### 3.2 Set-up

The river network is modelled as a collection of  $N$  river segments. We label these  $R_i$ , where  $i$  ranges from 1 to  $N$ , and construct a directed graph  $G = (R, E)$ , where  $R$  is its vertex set and  $E$  is its edge set. The vertices of  $G$  correspond to river segments, so  $R = \{R_i : i = 1, \dots, N\}$ .  $G$  has a directed edge  $\{R_i R_j\} \in E$  if segment  $R_i$  flows directly into segment  $R_j$ . See Figure 2 for an example.

For computational simplicity, segments are modelled as having a rectangular cross-section with widths  $w_i$ , slopes  $S_i$ , and lengths  $l_i$ . Here  $S_i = \tan(\theta_i)$  where  $\theta_i$  is the average angle the river bed makes with the horizontal. An important property of a leaky dam is that it has minimal impact when the flow is small. To get this behaviour, we closely follow the method in Hankin et al, 2020, where dams are  $H_u$  m tall but have a gap of height  $H_l$  m under which water flows without restriction, as shown in Figure 3. The variable  $h$  measures the height of water behind the dam, and the variable  $h_{stream}$  measures the

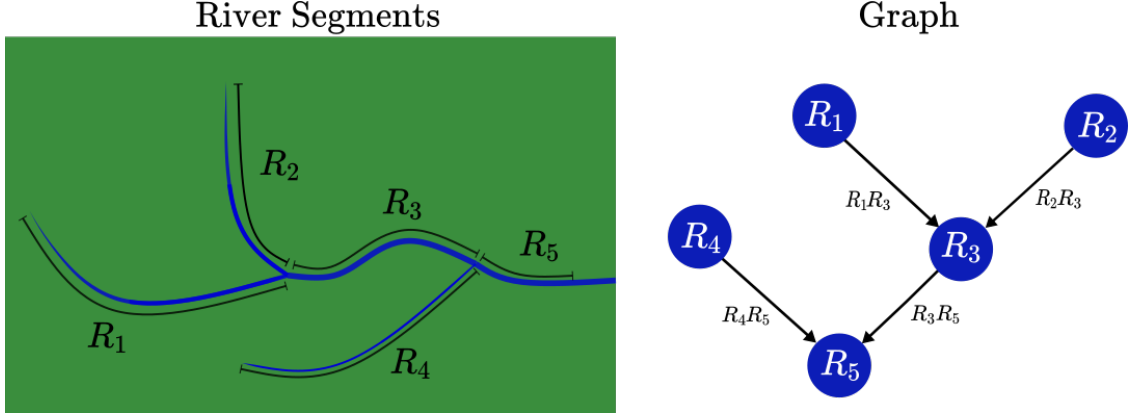


Figure 2: Example river network and corresponding directed graph.

height of water downstream from the dam. Table 19 is a summary of all of the variables used in this section.

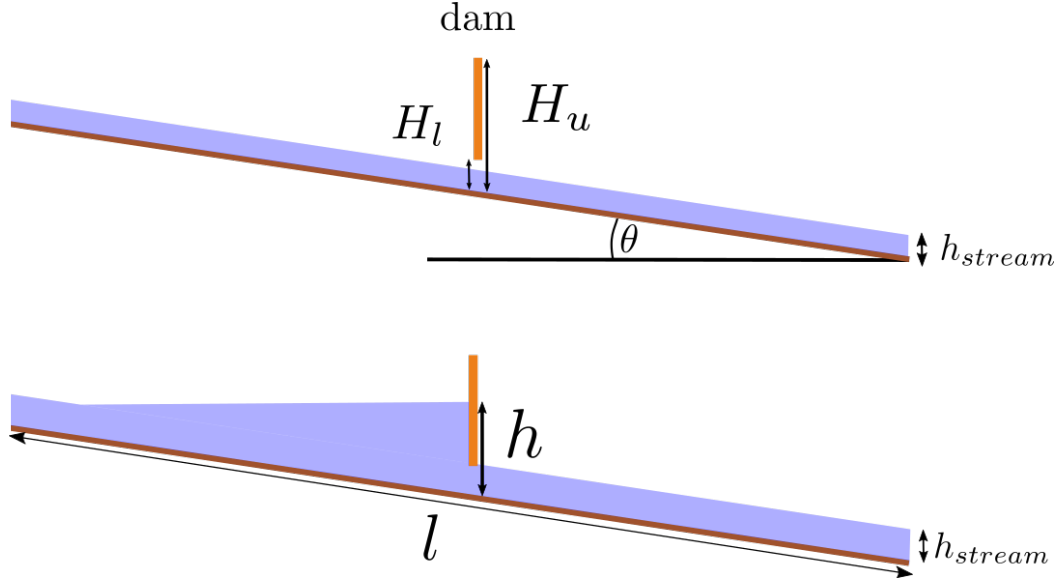


Figure 3: Segment profile with dam for two different flows

### 3.3 Governing Equations

For each river segment  $R_i$ , we define  $V_i$  as the total volume of water it contains and  $Q_i$  as the flow leaving it. Let  $q_i(t)$  be the inflow into  $R_i$  at time  $t$  - this models inflow from rain and groundwater, and in applications will have to be measured or modelled using over-land rain models, for example see Metcalfe et al, 2017. Conservation of mass gives the differential equation

$$\frac{dV_i}{dt} = \sum_j Q_j - Q_i + q_i(t)$$

for each segment, where the sum is over all edges of the form  $R_j R_i$  (i.e. all segments that flow directly into segment  $R_i$ ). This system can then be written as

$$\frac{d\mathbf{V}}{dt} = A^\top \mathbf{Q} - \mathbf{Q} + \mathbf{q}(t) \quad (4)$$

where  $\mathbf{V} = (V_1, \dots, V_N)$ ,  $\mathbf{Q} = (Q_1, \dots, Q_N)$ ,  $\mathbf{q}(t) = (q_1(t), \dots, q_N(t))$ , and  $A$  is the adjacency matrix of the graph  $G$ .

In order to solve this,  $\mathbf{Q}$  and  $\mathbf{V}$  need to be related.  $Q_i$  can be calculated as a function of  $h_i$  with widely used empirical formulae. The following formulae are from Munson et al, 2006, and for this section the subscripts  $i$  are temporarily dropped for simplicity.

Free flow in a rectangular channel with hydraulic radius  $r_h$  is given by

$$Q = \frac{1}{n} wh r_h^{2/3} \sqrt{S}, \quad r_h = \frac{wh}{w + 2h}. \quad (5)$$

This is an empirical formula that involves the Manning coefficient  $n$  - a measure of how ‘rough’ part of a river is. A discussion on finding the correct values for a given application can be found in Chow, 1985. A simplification to this formula is to make a hydraulic assumption that  $h$  will be small compared to  $w$ , so  $w + 2h \approx w$  (Hewitt, 2020). Under this assumption, the relation is

$$Q = \frac{1}{n} wh^{5/3} \sqrt{S}. \quad (6)$$

Flow under a sluice gate is given by Bernoulli’s equation

$$Q = w \sqrt{2g} \frac{h H^l}{\sqrt{h + H^l}}, \quad (7)$$

where  $H^l$  is the distance between the channel bottom and the bottom of the sluice and  $g \approx 9.8 \text{ m s}^{-2}$  is acceleration due to gravity.

Flow over a weir is given by

$$Q = C_{wr} \frac{2}{3} \sqrt{2g} w \max(0, h - H^u)^{3/2}, \quad (8)$$

where  $H^u$  is the weir height and  $h$  is the downstream height.  $C_{wr}$  is the weir coefficient, taken here to be 0.6 (Munson et al, 2006).

Since the dams being modelled are leaky, they should also be at least somewhat permeable. This could be achieved with a permeability term of the form

$$Q = kw \sqrt{2gh} \min(h - H_l, H_u - H_l) . \quad (9)$$

This depends on a non dimensional permeability constant  $k$ . Since there is a lack of data to compute a reasonable value for this, I ignore this term and take  $k = 0$  from here on. It is however kept in the equations for completeness.

Which of these relations is appropriate for  $Q$  depends on the river height at the dam  $h$ . From above, there are two different predictions for flow through the leaky dam. Friction limited flow, from (5):

$$Q_{fric}(h) = \frac{1}{n} wh^{5/3} \sqrt{S} \quad (10)$$

and dam limited flow:

$$Q_{dam}(h) = w\sqrt{2g} \left[ \frac{H^l h}{\sqrt{h + H_l}} + k\sqrt{h} \min(h - H^l, H^u - H^l) + \frac{2}{3} \max(0, h - H^u)^{3/2} \right]. \quad (11)$$

Dam limited flow is found as the sum of Equations 7, 8 and 9.

Also note that the dam can only limit the flow if  $h \geq H^l$ . This means that care needs to be taken when deciding which flow value to use. Note in general  $Q_{fric}(H^l) \neq Q_{dam}(H^l)$ . This is expected, as the formulae come from different empirical sources. However, this is also consistent theoretically as the base of the dam will impact stream flow due to viscosity.

- If  $Q_{fric}(H_l) \geq Q_{dam}(H_l)$  then the dam immediately assumes hydraulic control when  $h$  exceeds  $H_l$  (There is decrease in flow as  $h$  rises past  $H_l$ ).
- If  $Q_{fric}(H_l) < Q_{dam}(H_l)$  then the flow is still friction limited, and the dam has yet to impact flow. There will be a critical value  $h_c$  (where  $h_c \geq H_l$ ) satisfying  $Q_{fric}(h_c) = Q_{dam}(h_c)$ .<sup>2</sup>

Defining a critical switching height  $h_{crit}$  for both cases

$$h_{crit} = \begin{cases} H_l & Q_{fric}(H_l) \geq Q_{dam}(H_l) \\ h_c & Q_{fric}(H_l) < Q_{dam}(H_l) \end{cases},$$

the flow through a dam can be expressed in terms of the height of water behind it  $h$ , as

$$Q^*(h) = \begin{cases} Q_{fric}(h) & h < h_{crit} \\ Q_{dam}(h) & h \geq h_{crit} \end{cases}. \quad (12)$$

Note  $Q^*(h)$  is a *function* whereas  $Q$  is the variable flow out of a segment, which is why the \* notation is added to distinguish them.

The volume of water in a segment is given by

$$V^*(h; h_{stream}) = \begin{cases} wh_{stream} + \frac{w}{2S} \max(0, h - h_{stream})^2 & h < h_{stream} + Sl \\ wl(h - \frac{1}{2}Sl) & h \geq h_{stream} + Sl \end{cases},$$

where  $h_{stream}$  is the height of the free flowing water in the segment. The first case is where the reservoir doesn't take up the length of the segment, and the second if the water has backed up behind the dam enough to fill the whole segment (see Figure 3).

---

<sup>2</sup> $Q_{fric}(h) \propto h^{5/3}$  whereas  $Q_{dam}(h) \propto h^{3/2}$

However, given examples of existing dams, this would underestimate the volume of water that can be stored behind a dam. This is due to the dam causing the stream to back up and burst its banks. To address this, we add a storage coefficient  $\lambda \geq 1$  which increases the volume of water that a dam can store.  $V^*$  is then

$$V^*(h; h_{stream}) = \begin{cases} wlh_{stream} + \lambda \frac{w}{2S} \max(0, h - h_{stream})^2 & h < h_{stream} + Sl \\ wlh_{stream} + \frac{\lambda}{2} wSl^2 + wl(h - h_{stream} - Sl) & h \geq h_{stream} + Sl \end{cases},$$

which is equivalent to

$$V^*(h; h_{stream}) = \begin{cases} wlh_{stream} + \lambda \frac{w}{2S} \max(0, h - h_{stream})^2 & h < h_{stream} + Sl \\ wl\left(h - (1 - \frac{\lambda}{2})Sl\right) & h \geq h_{stream} + Sl \end{cases}. \quad (13)$$

To use this,  $h_{stream}$  needs to be found. Inverting Equation 6 with  $Q = Q^*(h)$  gives

$$h_{stream}(h) = \left( \frac{nQ^*(h)}{w\sqrt{S}} \right)^{3/5}. \quad (14)$$

Note that in the case  $Q^* = Q_{fric}$  in (12), this gives  $h_{stream} = h$ . When  $Q^* = Q_{dam}$ ,  $h_{stream} \leq h$ . Taking  $V^*(h) = V^*(h, h_{stream}(h))$  makes  $V$  a function of  $h$  only.

### 3.4 Nondimensionalisation

The variables  $w$ ,  $l$ ,  $h$ ,  $S$ ,  $Q$ ,  $V$ ,  $t$  will be nondimensionalised. Dimensionless constant scales  $\alpha$  and  $\beta$  are also defined. The constants are denoted with a subscript  $c$  (e.g.  $V_c$ ) and the nondimensional variables with hats (e.g.  $\hat{V}$ ).

$$t = t_c \hat{t} \quad l = l_c \hat{l} \quad w = w_c \hat{w} \quad h = h_c \hat{h} \quad S = S_c \hat{S} \quad V = V_c \hat{V} \quad Q = Q_c \hat{Q}$$

To determine appropriate nondimensional constants,  $l_c$ ,  $w_c$ ,  $h_c$  and  $S_c$  should be taken to correspond roughly to their average values for a specific, and then balancing terms in the equations suggests defining

$$Q_c = w_c h_c^{3/5} \sqrt{S_c}, \quad t_c = \frac{l_c w_c h_c}{Q_c}, \quad V_c = l_c w_c h_c, \quad \alpha = \frac{w_c h_c^{3/2} \sqrt{2g}}{Q_c}, \quad \beta = \frac{h_c}{l_c S_c}.$$

The problem now becomes:

$$\frac{d\hat{V}}{d\hat{t}} = A^\top \hat{Q} - \hat{Q} + \hat{q}(\hat{t}), \quad (15)$$

where, for each segment  $i$ ,

$$\hat{Q}^*(h) = \begin{cases} \frac{1}{n} wh^{5/3} \sqrt{S} & h < \hat{h}_{crit} \\ \alpha w \left[ \frac{H^l h}{\sqrt{h + H_l}} + \cdot \frac{2}{3} \max(0, h - H^u)^{3/2} \right] & h \geq \hat{h}_{crit} \end{cases}, \quad (16)$$

$$\hat{V}^*(h) = \begin{cases} \hat{w}\hat{l}\hat{h}_{stream} + \frac{1}{\beta} \lambda \frac{\hat{w}}{2\hat{S}} \max(0, h - \hat{h}_{stream})^2 & h < \hat{h}_{stream} + \beta \hat{S}\hat{l} \\ \hat{w}\hat{l}\left(h - \beta(1 - \frac{\lambda}{2})\hat{S}\hat{l}\right) & h \geq \hat{h}_{stream} + \beta \hat{S}\hat{l} \end{cases}, \quad (17)$$

$$\text{and } \hat{h}_{stream} = \left( \frac{n\hat{Q}^*(h)}{\hat{w}\sqrt{\hat{S}}} \right)^{3/5}.$$

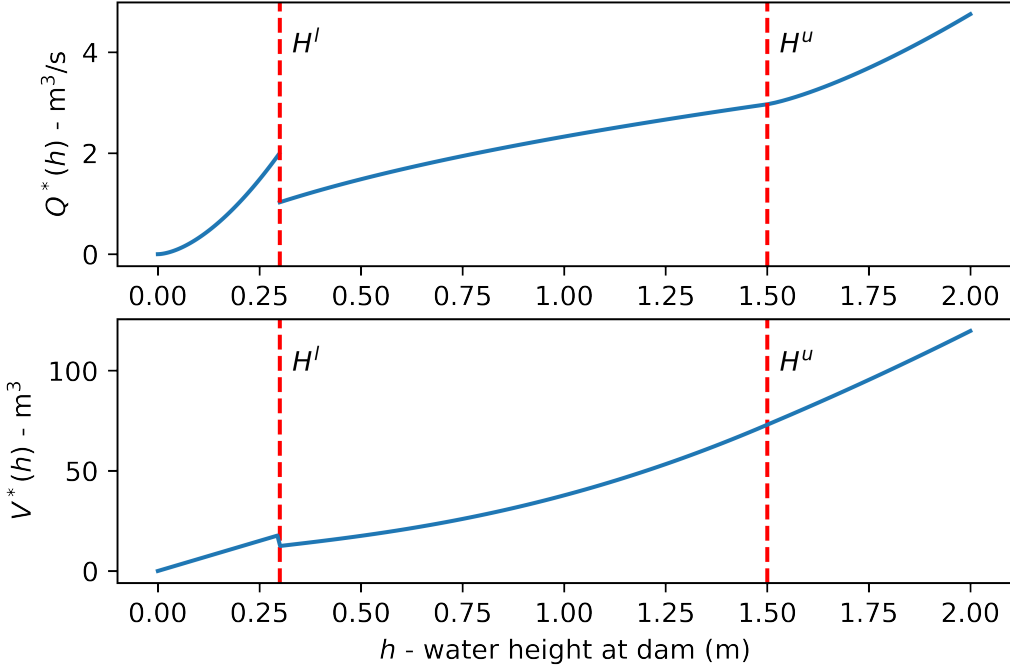


Figure 18: Example plots of  $Q^*$  and  $V^*$  showing potential non-monotonicity at  $H^l$ . Here,  $l=50\text{m}$ ,  $w=2\text{m}$ ,  $S=0.05$ .

$l_i$	Length	$H_i^l$	Lower dam height
$w_i$	Width	$H_i^u$	Upper dam height
$S_i$	Slope	$k_i$	Dam permeability
$h_i$	River height at dam	$\lambda_i$	Dam storage coefficient
$n_i$	Manning (roughness) coefficient	$h_{stream}(h)$	Downstream height function
$V_i$	Volume of water in segment	$Q_i^*(h)$	Flow function
$q_i(t)$	Inflow at time t	$V_i^*(h)$	Volume function
$A$	Adjacency matrix of $G$		
$\mathbf{V}$	$(V_1, V_2, \dots, V_N)^\top$		
$\mathbf{Q}$	$(Q_1, Q_2, \dots, Q_N)^\top$		
$\mathbf{h}$	$(h_1, \dots, h_N)^\top$		
$\mathbf{V}^*(\mathbf{h})$	$(V_1^*(h_1), \dots, V_N^*(h_N))^\top$		
$\mathbf{Q}^*(\mathbf{h})$	$(Q_1^*(h_1), \dots, Q_N^*(h_N))^\top$		
$\mathbf{q}(t)$	$(q_1(t), \dots, q_N(t))^\top$		

Table 19: Notation

### 3.5 Computational Approaches

There are different possible methods to solve the system of ODEs (15). One approach is to try and express  $\mathbf{Q}$  as a function of  $\mathbf{V}$ , for example by finding an inverse to  $\mathbf{V}^*(\mathbf{h})$  (say  $\mathbf{f}(\mathbf{V})$ ) and setting  $\mathbf{Q} = \mathbf{Q}^*(\mathbf{f}(\mathbf{V}))$ . However,  $\mathbf{Q}$  is not necessarily monotone increasing, and  $\mathbf{V}$  depends on  $\mathbf{Q}$  via  $h_{stream}$ . A monotone approximation can be used, which although

it is computationally efficient, may lose accuracy especially if  $h_i \approx H_i^l$  for some  $i$ . This is one possible (efficient) method.

A potential issue with this method is that differential equations can lead to hysteresis - this is the dependence of a solution on its previous states. This comes from the potential non-monotonicity of  $Q^*(h)$ , as there may be multiple solutions to  $Q^*(h) = Q_0$  if  $Q_0$  is chosen appropriately.

An approach which allows for this possibility is to add a differential equation for  $\mathbf{h}$ . The following system of  $2N$  variables will give the correct behaviour, where  $\varepsilon \geq 0$  is a small constant:

$$\varepsilon \frac{d\hat{\mathbf{h}}}{dt} = \hat{\mathbf{V}} - \hat{\mathbf{V}}^*(\hat{\mathbf{h}}) \quad (20)$$

$$\frac{d\hat{\mathbf{V}}}{dt} = A^\top \hat{\mathbf{Q}}^*(\hat{\mathbf{h}}) - \hat{\mathbf{Q}}^*(\hat{\mathbf{h}}) + \hat{\mathbf{q}}(\hat{t}) \quad (21)$$

This needs some explanation. Note that the difference between  $\hat{\mathbf{V}}$  and  $\hat{\mathbf{V}}^*(\hat{\mathbf{h}})$  is critical here. Both equations are defined on the nondimensionalised variables. Because of this, taking  $\varepsilon$  to be small makes  $\hat{\mathbf{h}}$  evolve on a faster timescale than  $\hat{\mathbf{V}}$ . For a fixed  $\hat{\mathbf{V}}$ , the stationary points of Equation 20 are values  $\mathbf{h}$  satisfying  $\hat{\mathbf{V}} = \hat{\mathbf{V}}^*(\mathbf{h})$ .

Note that this sidesteps the problem of inverting  $\hat{\mathbf{V}}^*(\hat{\mathbf{h}})$ , and deals with the potential non-monotonicity of  $\hat{\mathbf{Q}}^*(\hat{\mathbf{h}})$ . A large disadvantage of this method is that equations (20), (21) have  $\mathbf{h}$  and  $\mathbf{V}$  vary on different timescales. This is a typical example of a stiff numerical problem - which will decrease the efficiency of a numerical solver. The specific value for  $\varepsilon$  should be chosen once the nondimensionalisation constants are set to make sure  $\mathbf{h}$  evolves on a faster timescale than  $\mathbf{V}$ .

### 3.6 Comparing Approaches

Of the two solver methods in the above section, the monotone approximation is significantly faster - how similar are it's predictions to the more theoretically accurate hysteresis model? This section will compare the two on a model problem. The code for these, as well as the code and data for the application, are available on GitHub<sup>3</sup>. This contains notebooks working through the implementation with example results. The plots below are using this code.

I will compare models on a small example network consisting of four segments in a line, that is  $G = (\{R_1, R_2, R_3, R_4\}, \{R_1R_2, R_2R_3, R_3R_4\})$ . These have  $l = 100\text{m}$ ,  $w = 2\text{m}$ ,  $S = 0.05$  and  $\lambda = 10$ , which represent a typical small river segment. Each segment has a leaky dam. The inflow is Gaussian in time into the first segment only. This would model an intermediate part of a river network undergoing an idealised flood. Here,  $H^u = 1.5\text{m}$  and  $H^l$  varies. Figure 22 shows the results for the water height  $h$  and flow  $Q$  downstream.

There are small differences in the height plots, but methods give very similar flow results. Flow is the more important result here. However, there are some situations where the models predict different results, where the numerical approximation doesn't capture the hysteresis of the problem. An example is shown in Figure 23. This uses the same parameters as above, with  $H^l = 0.2$ , but a different rain inflow. In this, the hysteresis model allows for two different steady states for  $h$  which give the same flow value. Note however that both models give the same flow results.

---

<sup>3</sup><https://github.com/robgondris/network-flood-model>

The plots in Figure 22 show the importance of determining a good value for  $H^l$ . If it is too low, for example Figure 22 a), then the dams will have already been filled up before the worst of the flood has reached them. This means that there will be minimal impact on the maximum flow value. However if  $H^l$  is too high, then it might not have any impact at all - if, for example, the river water height never reaches it.

For networks modelling small catchments, so with small flow values, this situation is less of an issue as the total volume that a dam set-up can store will be of a similar order to the total volume of water that flows through the network during the course of a flood. However, when designing a dam set-up for a larger network care needs to be taken to ensure the dams only impact near the peak of a flood. This is illustrated in Section 4.4.

### Flow and Height plots for $R_4$

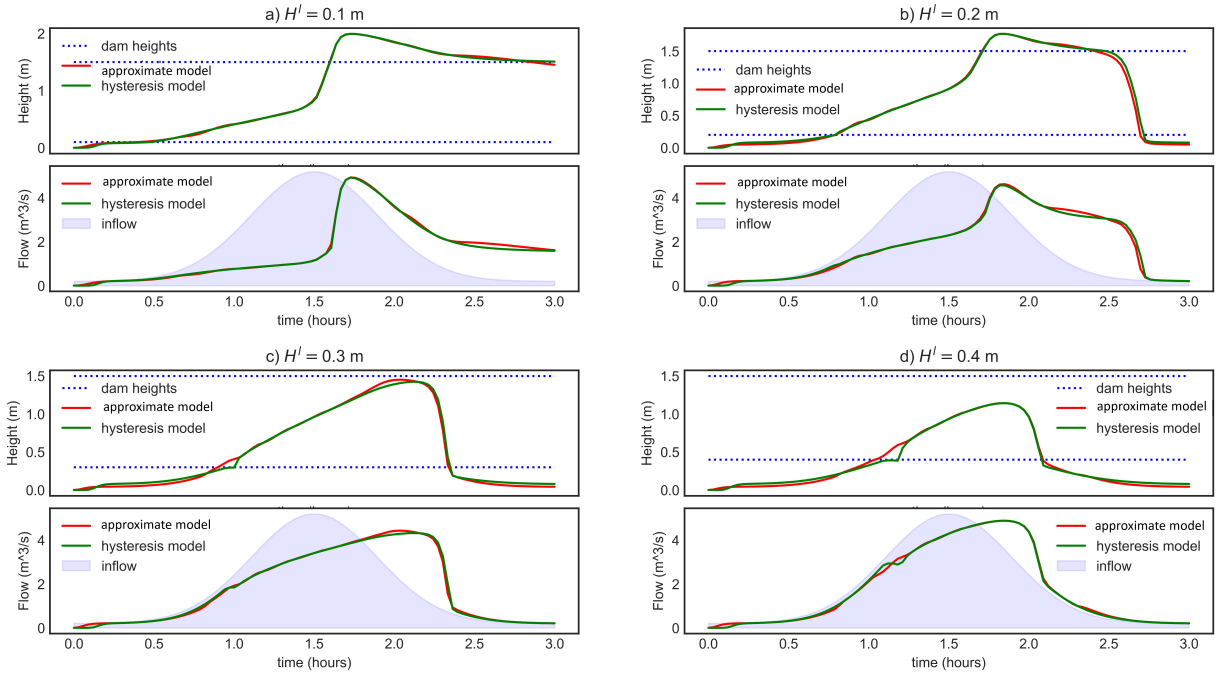


Figure 22: Comparing Methods, segment details given in 3.6. Horizontal blue dotted lines are  $H^l$  and  $H^u$

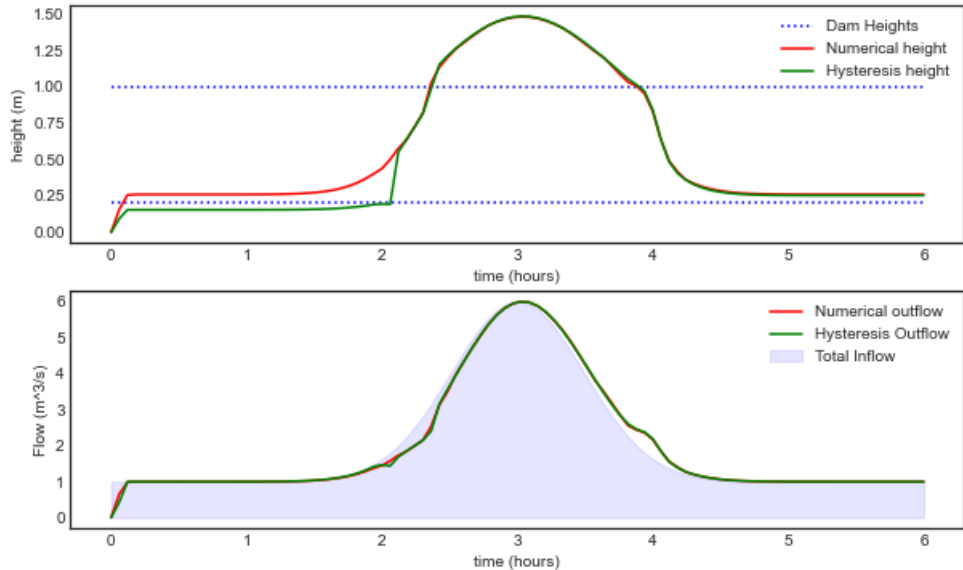


Figure 23: Water height and flow rate for  $H^l = 0.2 \text{ m}$ , as in Figure 22 but with a larger base inflow

## 4 Application

In this section, we apply the model to a large network to assess the potential effectiveness of building dams here. The location was suggested by Barry Hankin from the JBA Trust, who also provided data on the network and a rainfall profile.

The river network is the catchment to Bowston in Cumbria, England and is shown in Figure 24. This catchment is the source of the river Kent, with a catchment area of 70.6 km<sup>2</sup>. The river Kent is prone to flooding downstream, for example it caused flooding in Kendal during storm Ciara in early February 2020 (BBC news, 2020 [10]). The South Cumbria Rivers Trust will start implementing Natural Flood Measures (of which Leaky Dams are a part of) as part of a DEFRA funded scheme to mitigate flooding [12]. Here we will assess the potential effectiveness of placing dams in the upper catchment.

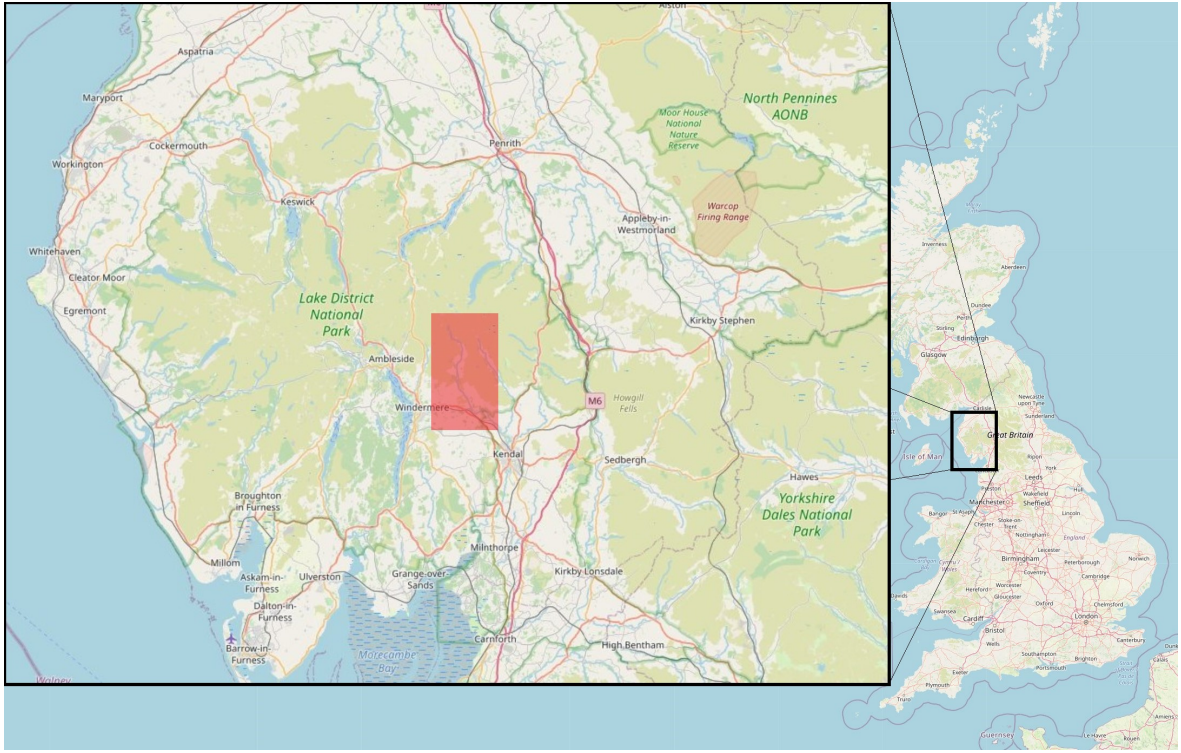


Figure 24: Catchment location, ©OpenStreetMap

### 4.1 Setup

Terrain and rainfall data is provided by Barry Hankin. Additionally, elevation data is used from the National LIDAR Programme [13]. The network is modelled as 1764 river segments, with every segment containing a dam. The dams are initially set to have  $H^l = 100\text{m}$ , meaning that under any realistic flow these dams will have no impact. A situation where  $h \geq 100\text{m}$  would certainly call for more drastic flood prevention measures! The network and its location is shown in Figure 25.

### 4.2 Rainfall Data

The rainfall data provided by Barry Hankin gives inflows into each segment, generated using a ‘dynamic topmodel’ (see Metcalfe et al, 2015). The data represents inflow into each



Figure 25: River Network.

segment, not rainfall - so this includes considerations of groundwater flow and overland flow. To check the accuracy of my model we use data from the Bowston gauge, provided by NRFA ([11]).

To check the data, Figure 26 a) shows the total inflow into the whole network and the measured outflow at Bowston gauge, the final segment of the network. Note these represent different values - one is inflow into the whole network, the other is outflow at the lowermost segment. However, it is expected that these would give similar plots especially since the values are plotted over several months. In particular, it's expected that their integrals will be equal if mass is conserved. However, it is clear that there is some discrepancy between the plots. Most notably, the total inflow is for long periods of time at  $0\text{m}^3/\text{s}$  which is unrealistic - the river Kent doesn't only flow during storms! This is further reinforced by the large difference in the total volumes of water each flow predicts. From 1<sup>st</sup> Jan 2020 to 29<sup>th</sup> Feb 2020, the inflow data shows a total volume of  $3.3 \times 10^7 \text{m}^3$ , whereas the Bowston gauge records a volume of  $5.3 \times 10^7 \text{m}^3$ . To improve the accuracy of the data the difference is added as a 'baseflow', representing inflow from groundwater and stored water which - it must be assumed - is missing from the modelled inflow. This

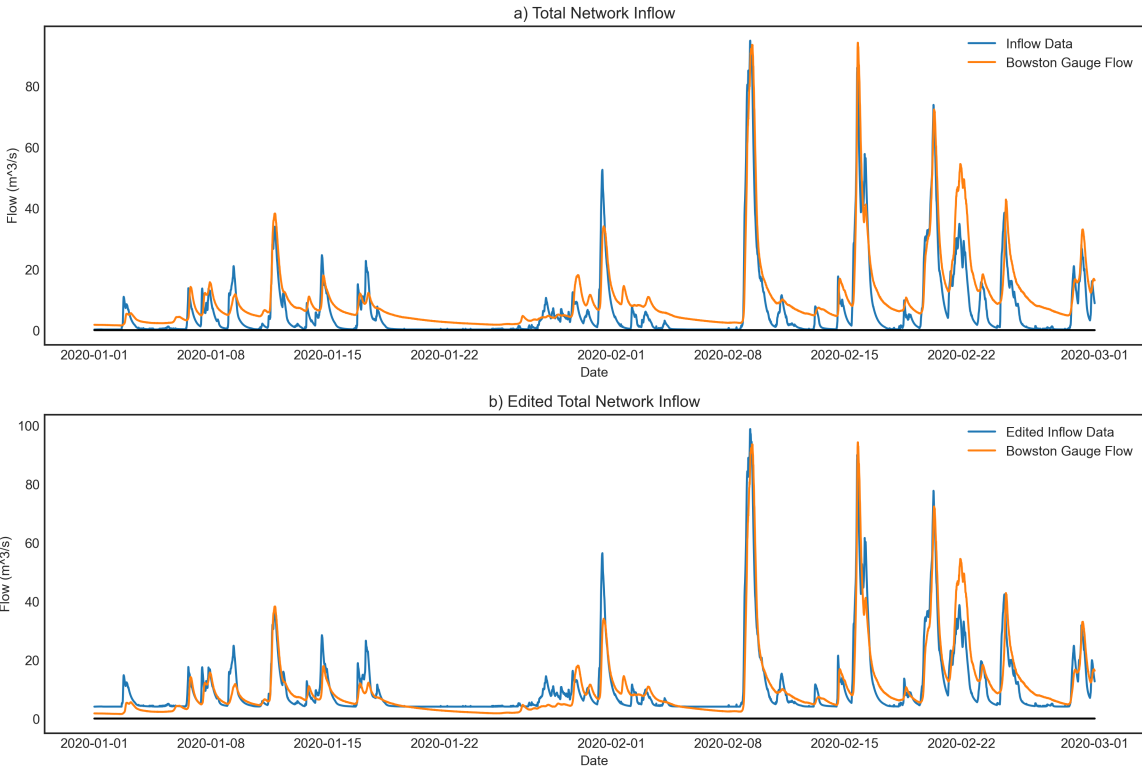


Figure 26: Plotting total network inflow and network outflow over time

difference is proportioned over the river network according to the length ratios  $\frac{l_i}{\sum_{j=1}^N l_j}$ . This is shown in Figure 26 (b).

### 4.3 Implementation

Both the approximate and hysteresis formulations are implemented in Python. Plots here will be from the approximate version due to its efficiency. The codes are presented with explanation and a worked through example in Jupyter notebooks on Github<sup>4</sup>. This also gives code on how to animate solutions so that the flow values over the whole network and details about the dam set-up can be visualised.

Additionally, as there is no available segment width data, values have been calculated from the existing data. A list of segments which could potentially contain a leaky dam has been calculated, as these can only be built on sufficiently small streams. See the notebooks for details. For the rest of this section we'll focus on storm Ciara, the peak of which is around the 9<sup>th</sup> Feb 2020.  $\lambda$  is taken to be 20.

### 4.4 Results

Figure 27 shows some results for the network. Figure 27(a) compares the predicted flow with the gauge readings. Plots (b) to (d) show the effect of different numbers of identically built dams with properties  $H^l = 0.3\text{m}$  and  $H^u = 1.5\text{m}$ . These dams are randomly placed on suitable branches of the network. For better visualisation, use the

<sup>4</sup><https://github.com/robgondris/network-flood-model>

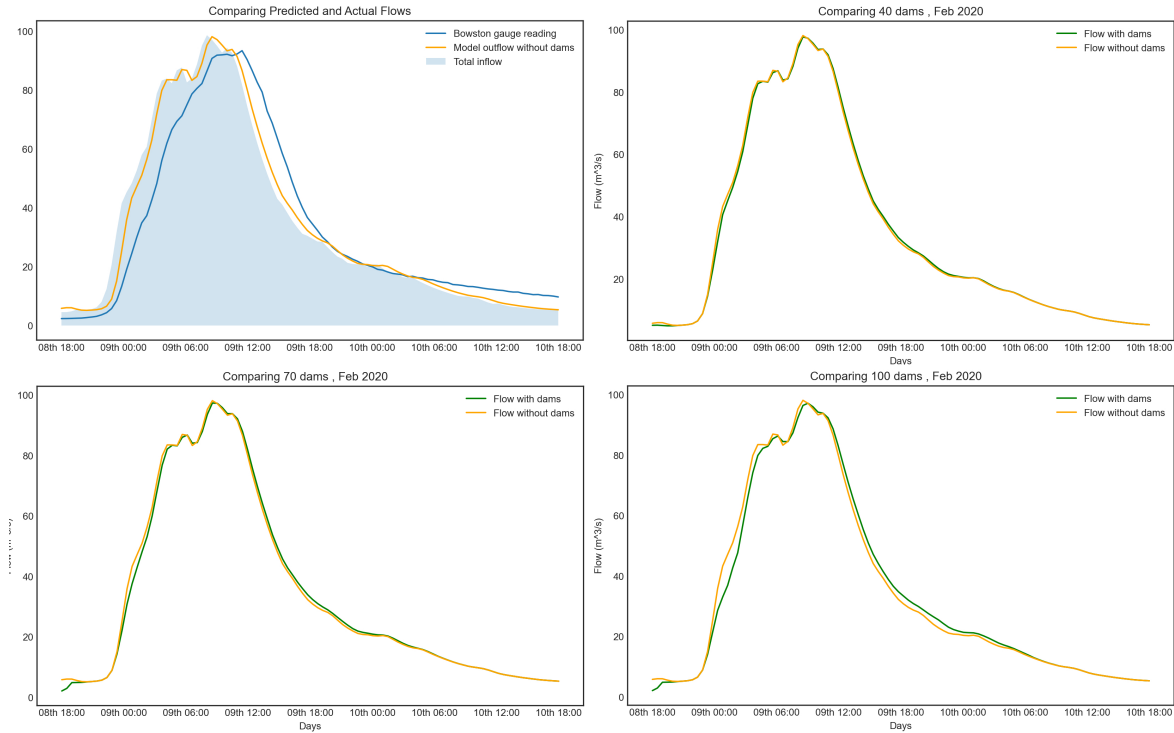


Figure 27: Uniform Dam Effectiveness

code is found in the GitHub repo<sup>5</sup>. For all cases there is little impact on the maximum flow even if there is some impact on other areas. This is due to the dams all being created identically, and so it is likely that they have little impact on the peak of the flood (either by not being filled at all or by filling completely before the peak has arrived, see Section 3.6). This can more clearly be seen in Figure 28, which plots how full each dam is as a percentage at a particular instant of time. There is a large range of problems - some have not had any impact at all, and others are completely full. This figure is animated through the GitHub code, the figure shows the state of the dams when the flow is maximal.

This problem is also clearly seen in Figure 27(d), where the dams have an impact when the flow is still relatively low, and therefore a much smaller impact near the maximum flow.

---

<sup>5</sup><https://github.com/robgonzales/network-flood-model>

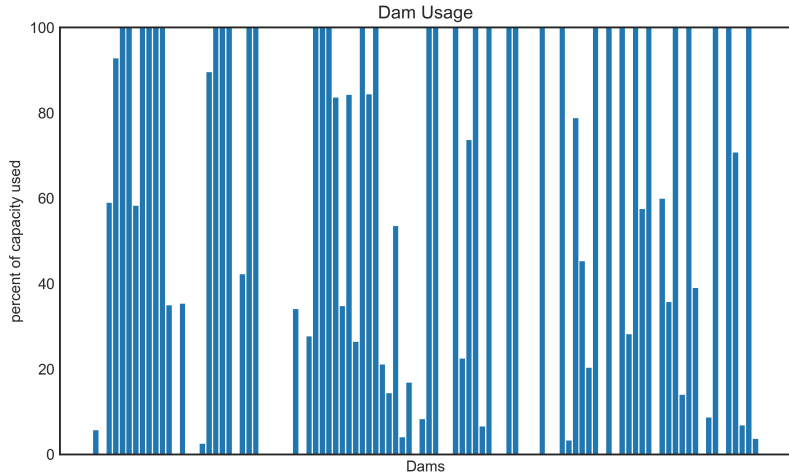


Figure 28: Dam capacity percentages at max flow for 27d)

This shows the need to design the dams in such a way that the majority of their impact is around the worst of the flood. One possible way of achieving this result is to first run a simulation with no dams, and for each segment calculate  $\gamma_i$ , the maximum height of the river over the course of the flood. Then for each dam set  $H_i^l = 0.85\gamma_i$ . This will make sure the dams all have an impact when the flood is near its peak. The results are shown in Figure 29. Dam usage is shown in figure 30. Using 100 dams with this approach decreases the the maximum flow by 3.7%, and for 200 dams there is a 5.9% decrease. This shows the value of designing the dams based on a model of the network with no dams. Also, the dams are used much more effectively, with almost all being used to their maximum capacity. However for this application, an unreasonable number of leaky dams are required to have a significant effect. This goes without considering the additional cost of designing these specific dams.

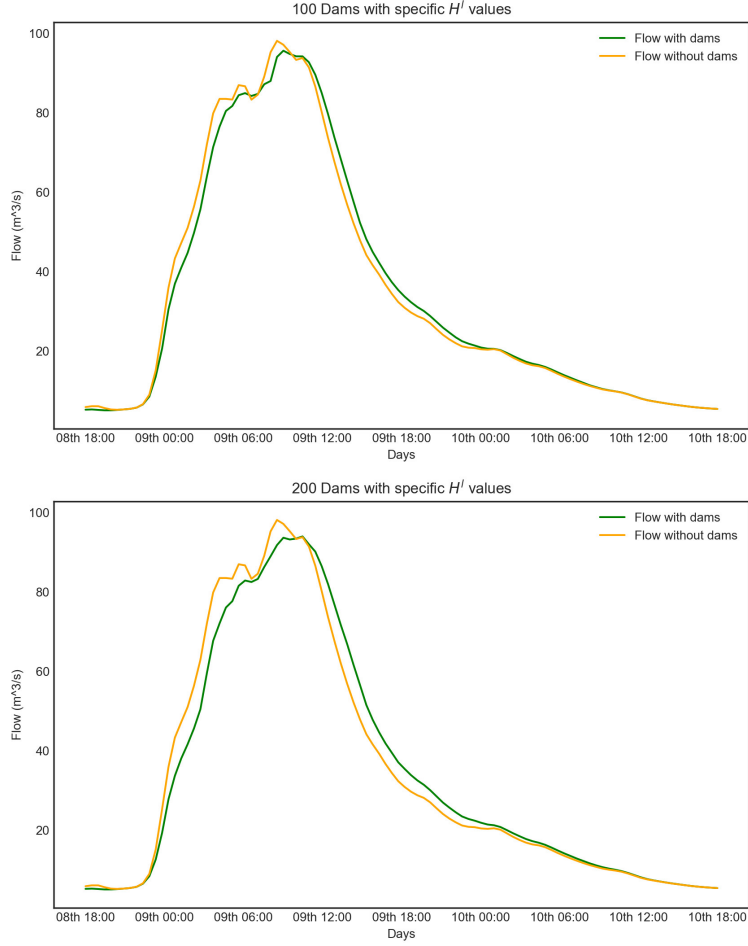


Figure 29: Dam Effectiveness where  $H^l = 0.85\gamma$

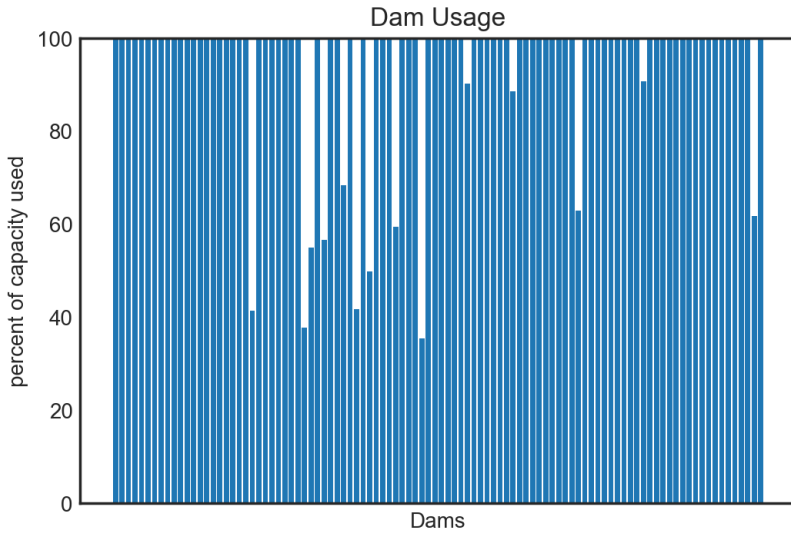


Figure 30: Dam capacity percentages at the time of maximum flow for reformulation in Figure 29(d))

If the dams have slightly different parameters, say  $H_i^l = 0.5\gamma_i$ , then there is a noticeable decrease in effectiveness as shown in Figure (31). This could easily happen if the dams

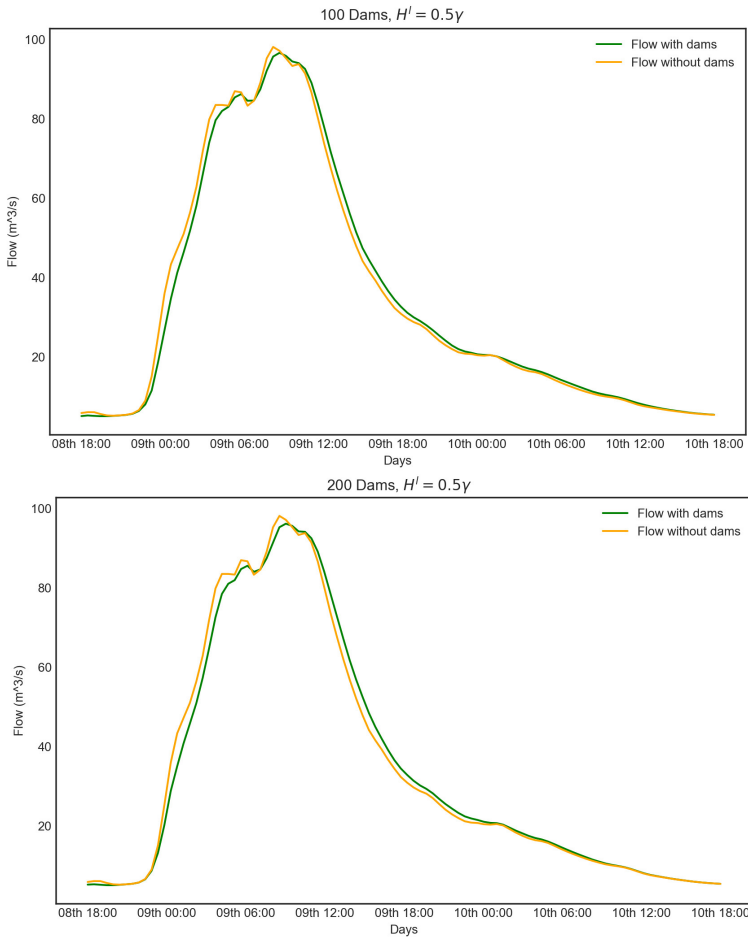


Figure 31: Dam Effectiveness where  $H^l = 0.5\gamma$

get partially blocked with debris, and as leaky dams wouldn't be maintained regularly. This is yet another difficulty that would need to be overcome.

These results are only for storm Ciara. When the dams are designed in this way, they will have different effects for different storms. Because the dams have been designed to start impacting when river heights reach 80% of Ciara's max height values, these dams will have minimal impact for smaller storms.

This is a general problem - any dam set-up designed this way will impact a specific range of floods. A similar procedure can be applied more generally with an analysis of expected peak flood values. As an example, the average yearly maximum flow value for Bowston is 64m<sup>3</sup>(NRFA [11]). A dam set-up can be constructed to impact floods of this height. However, this would only impact similar floods - it would have had minimal impact on the peak flow during storm Ciara for example. Having different dams to deal with different potential floods is a potential solution to this, but it would drastically increase the amount of dams that would have to be built.

## 4.5 Smaller Catchment

In previous papers the catchment size has been much smaller, where the volume stored by dams is of a similar order to the total volume of inflowing water during a flood. This means that determining when a dam acts is far less important. To show this, a small

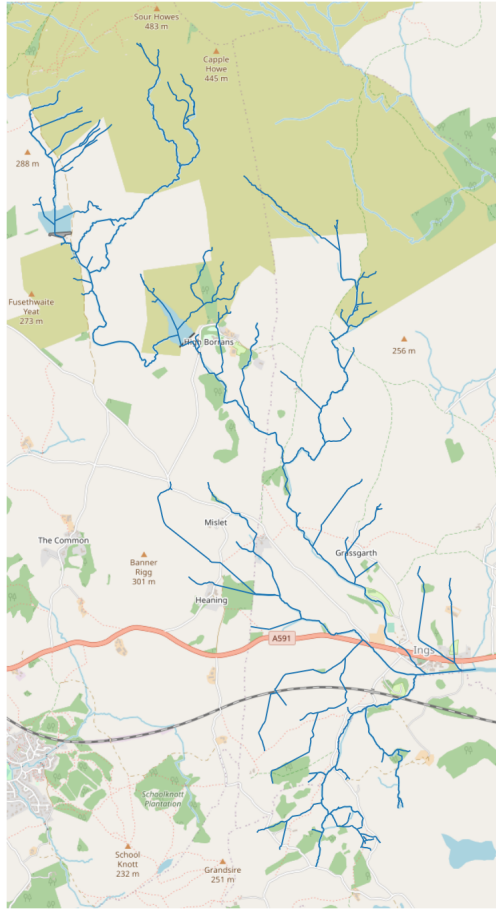


Figure 32: Smaller Network

subsection of the larger network is taken, shown in Figure 32. Plots for different dam set-ups are shown in Figures 33 and 34. Figure 33 compares uniformly constructed dams against designed dams. A uniform setup reduces maximum flow by 3.8%, whereas the designed dams reduce maximum flow by 4.7%.

Figure 34 compares how a different number of dams affect the flow. For 20, 40, 60 and 80 dams, the respective percentage decreases in max flow are 5.5, 6.9, 8.6 and 10.5%. This shows leaky dams can have a significant impact on smaller catchments.

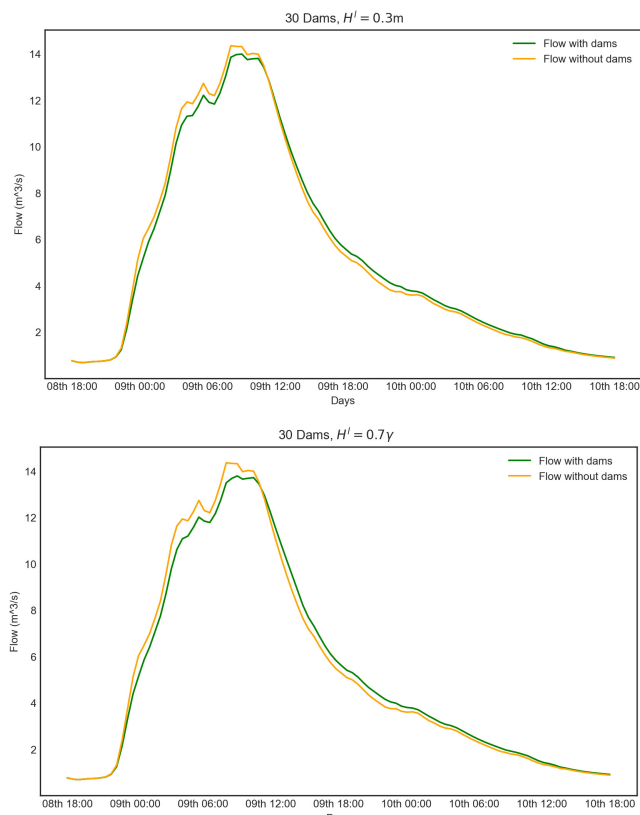


Figure 33: Comparing uniform dams to calculated dams

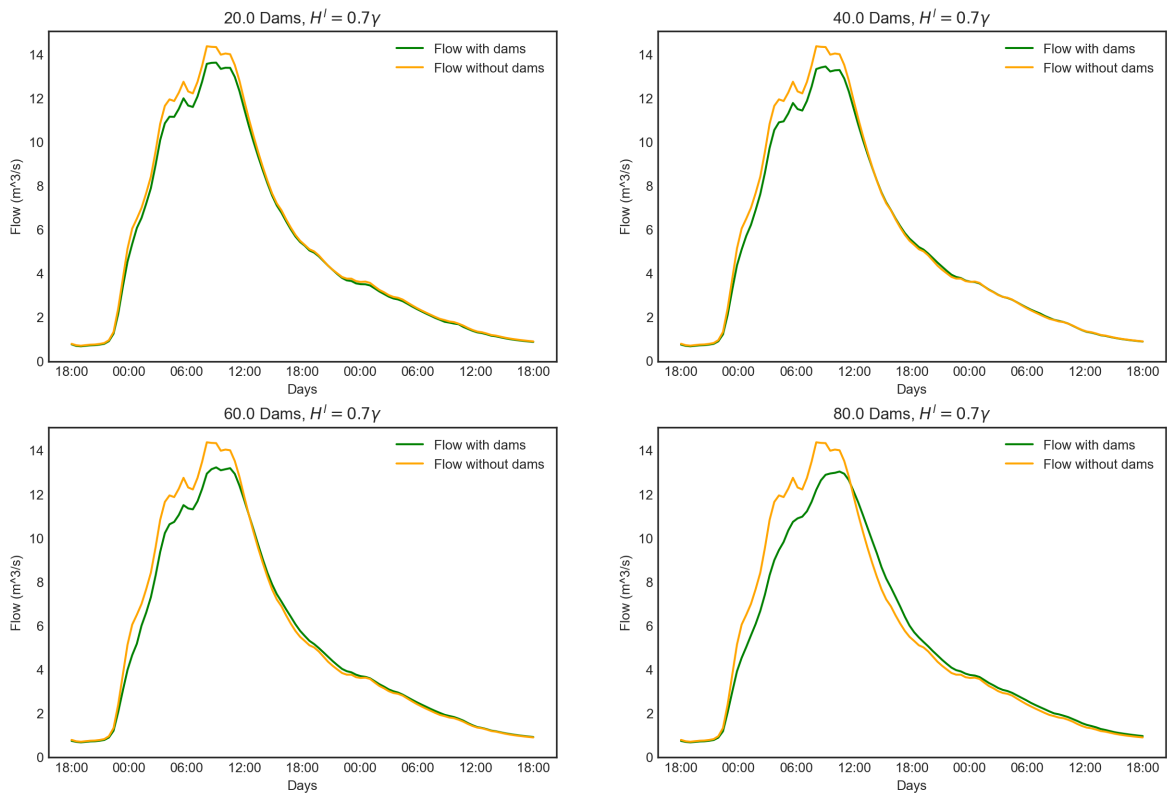


Figure 34: Comparing Number of Dams

## 5 Conclusion

In this project, we have derived a network-based differential equation model for calculating the effect of leaky dams on river flow. We have written code that implements the full formulation and also a numerical approximation that is accurate and more efficient, which can be applied to any suitable network. We then applied this to a network of 1764 segments, modelling a catchment of  $71 \text{ km}^2$ , and also to a smaller section of this. We find that on a small network leaky dams are effective. However on a larger network, simulations are necessary, as a random placement of identical dams will likely have no effect on the maximum flow during a flood. Using the model, dams can be constructed with parameters depending on their individual location, increasing their effectiveness significantly. However the number of dams needed to have a meaningful impact is large, and I've also shown that small errors in the specifics of each dam leads to large decreases in effectiveness.

Overall leaky dams have the potential to be effective for larger catchments, however this requires a large number of them which are all built to specifications depending on their position in the river network.

## 6 Acknowledgements

This project was funded by an LMS Undergraduate Research Bursary and by Oxford University Mathematical Institute. I would like to thank my supervisor Prof. Ian Hewitt, whose help, insights and guidance were invaluable. I would also like to thank Barry Hankin and Rob Lamb from the JBA Trust who provided detailed data and many helpful suggestions.

## References

- [1] Hankin, B., Hewitt, I., Sander, G., Danieli, F., Formetta, G., Kamilova, A., Kretzschmar, A., Kiradjiev, K., Wong, C., Pegler, S., and Lamb, R.: A risk-based network analysis of distributed in-stream leaky barriers for flood risk management, *Nat. Hazards Earth Syst. Sci.*, 20, 2567–2584, <https://doi.org/10.5194/nhess-20-2567-2020>, 2020
- [2] Environment Agency (2020) *Working with natural processes to reduce flood risk* Available at: <https://www.gov.uk/government/publications/working-with-natural-processes-to-reduce-flood-risk> (Accessed: 1 September 2020)
- [3] Nicholson A, O'Donnell G, Wilkinson M, Quinn P *The potential of runoff attenuation features as a Natural Flood Management approach* *J Flood Risk Management*. 2020; 13 ( Suppl. 1):e12565. <https://doi.org/10.1111/jfr3.12565>
- [4] HM Government (2018) *A Green Future: Our 25 Year Plan to Improve the Environment* Available at: [https://assets.publishing.service.gov.uk/government/uploads/system/uploads/attachment\\_data/file/693158/25-year-environment-plan.pdf](https://assets.publishing.service.gov.uk/government/uploads/system/uploads/attachment_data/file/693158/25-year-environment-plan.pdf) (Accessed: 1 September 2020)

- [5] Metcalfe P, Beven K, Hankin, B, Lamb R *Simplified representation of runoff attenuation features within analysis of the hydrological performance of a natural flood management scheme*. Hydrology and Earth System Sciences Discussions (<https://doi.org/10.5194/hess-2017-398>)
- [6] Follett, E, Schalko, I, Nepf, H. (2020) *Momentum and energy predict the back-water rise generated by a large wood jam*. Geophysical Research Letters, 47, e2020GL089346. (<https://doi.org/10.1029/2020GL089346>)
- [7] Munson R, Young D, Okiishi, T.H. (2006). *Fundamentals of fluid mechanics*. Hoboken, Nj: Wiley and Sons.
- [8] Chow, V., 1985. *Open-Channel Hydraulics*. Auckland: McGraw-Hill.
- [9] Hewitt I, (2019) *Mathematical Geoscience*, lecture notes, University of Oxford 2019 [https://courses.maths.ox.ac.uk/node/view\\_material/39483](https://courses.maths.ox.ac.uk/node/view_material/39483) (Accessed 25 August 2020)
- [10] BBC News (2020) *Storm Ciara: Residents battle to save homes from floodwaters*. Available at: <https://www.bbc.co.uk/news/uk-england-cumbria-51433960> (Accessed: 1 September 2020)
- [11] Environment Agency (2020) *National River Flow Archive, Kent at Bowston* Available at: <https://nrfa.ceh.ac.uk/data/station/info/73017> (Accessed 1 September 2020)
- [12] SCRT, 2020 *Kendal Town View Fields – NFM project* Available at: <https://scrt.co.uk/what-we-do/current-projects/natural-flood-management/kendal-nfm-project> (Accessed 1 September 2020)
- [13] Environment Agency, 2020 *National LIDAR Programme* Used with an open government licence <http://www.nationalarchives.gov.uk/doc/open-governmentlicence/version/3/> Available at <https://data.gov.uk/dataset/f0db0249-f17b-4036-9e65-309148c97ce4/national-lidar-programme>
- [14] Metcalfe, Peter, Beven, Keith, Freer, Jim (2015). *Dynamic TOPMODEL: A new implementation in R and its sensitivity to time and space steps*. Environmental Modelling and Software. 72. 155-172. 10.1016/j.envsoft.2015.06.010.